J. Fluid Mech. (1973), *vol.* 58, *part* 2, *pp.* 209–231
Printed in Great Britain

Turbulent source flow between parallel stationary and co-rotating disks

By E. BAKKE†, J. F. KREIDER AND F. KREITH
Department of Chemical Engineering, University of Colorado, Boulder

(Received 19 November 1972)

The research summarized in this paper is an experimental study of the velocity and turbulence fields in the gap between two parallel co-rotating or stationary disks with a source in the centre. Detailed hot-wire measurements over a wide range of source strengths and disk speeds are presented; the average velocity components are correlated in terms of dimensionless quantities; and the radial pressure distribution is analysed. Also, transition phenomena and conditions under which similarity in the velocity profiles can be expected are discussed.

1. Introduction

In flow between two parallel co-rotating disks with a source in the centre a velocity component exists in the tangential direction owing to the shear created by the moving disks while the centrifugal force acts radially outward on the fluid close to the disk. At any radius the tangential velocity component decreases with increasing distance from the disk surface. The average radial velocity decreases with increasing radial distance from the source since the flow is through an increasing cross-sectional area. The combination of the outward radial and tangential velocity components produces a spiral flow field in which the velocity vector changes its angle with the radius vector as the disk gap is traversed. The velocity vector is in the tangential direction (i.e. normal to the radius vector) at the rotating disk surface and turns towards the radius vector as the centre of the disk gap is approached. Also, since the radial velocity component decreases with radius in any plane, the fluid particles undergo a spiral-like motion as they move outward.

In flow between two parallel stationary disks with a source in the centre the fluid decelerates, resulting in an adverse pressure gradient. Also, inertial forces are generally larger than the viscous forces in such a configuration and the static pressure increases from the centre of the disk to the rim. As a result, separation may occur if the pressure gradient becomes sufficiently great.

The objective of this investigation was to study source flow between two parallel stationary or co-rotating disks. Specifically, this paper presents: (i) detailed hot-wire measurements of the flow field between stationary and co-rotating disks over a wide range of source strengths and disk speeds; (ii) a correlation of the average velocity components in terms of dimensionless variables; and (iii) an analysis of the radial pressure distribution.

† Present address: Director of Research and Development, Pulverizing MikroPul, Division of Slick Corp., Summit, New Jersey.

For a general survey of fluid mechanics in rotating systems the reader is referred to Dorfman (1963), Kreith (1968) and Greenspan (1968). The following review is limited to material related to source flow between two parallel stationary or co-rotating disks. When the Reynolds number in source flow between two disks becomes so small that the inertial forces can be neglected compared with the viscous forces, 'creeping flow' exists with a dimensionless radial velocity $U/U_h = 2(z/h)(1-z/2h)$, where z is the axial (vertical) distance and the distance between the disks is $2h$(ft). The pressure distribution in creeping flow was obtained by Licht & Fuller (1954). For higher Reynolds numbers when the inertia terms cannot be neglected, Osterle, Chou & Saibel (1957) and Livesey (1960) obtained approximate solutions for laminar flow by an integral method, but Savage (1964) obtained a better approximation by perturbing the creeping-flow solution. Moller (1963) measured the pressure distribution for laminar and turbulent flow, at disk gap-to-diameter ratios less than 0·0111 and exit Reynolds numbers above 500. Hagiwara (1962) studied the outward flow in a narrow radial diffuser and applied his results to the analysis of a pneumatic micrometer, where the disk spacing is less than 0·01 in.

Laminar source flow between two parallel co-rotating disks has been studied by Breiter & Pohlhausen (1962), Rice (1963), Peube & Kreith (1966), Matsch & Rice (1968) and Adams & Rice (1970). Breiter & Pohlhausen solved the linearized momentum equations analytically and the nonlinear equations approximately by a numerical technique whereas Peube & Kreith and Matsch & Rice all solved the complete momentum equation with a fixed source flow rate as one of the boundary conditions.

Daily & Nece (1960) measured velocity profiles and torques for a disk rotating in a housing. Daily, Ernst & Asbedian (1964) studied the influence of a source flow on the flow around a disk rotating in an enclosure and presented a theoretical analysis to predict the torque and the pressure distribution. Kreith, Doughman & Kozlowski (1963) studied flow transition and mass transfer from an enclosed rotating disk with and without source flow. No experimental results on source flow between two parallel co-rotating disks have yet been published.

2. Apparatus and experimental procedure

2.1. *Apparatus*

The experimental programme included mean velocity and turbulent intensity traverses in the radial and tangential directions and pressure measurements at different radial positions for various disk gaps, disk speeds and source flow rates.

The apparatus used for the experiment is shown in figure 1. Two smooth disks 22 in. in diameter were mounted parallel to each other with metered air entering through a hole in the centre of the lower disk. The disks rotated together by the action of a coupling. The disk spacing, rotational speed and source flow rate could be adjusted from 0 to 0·5 in., from 0 to 2000 r.p.m. and from 0 to 100 ft^3/min, respectively.

Velocity measurements were taken with a two-channel constant-temperature hot-wire anemometer described by Berger, Freymuth & Frobel (1963) and Frey-

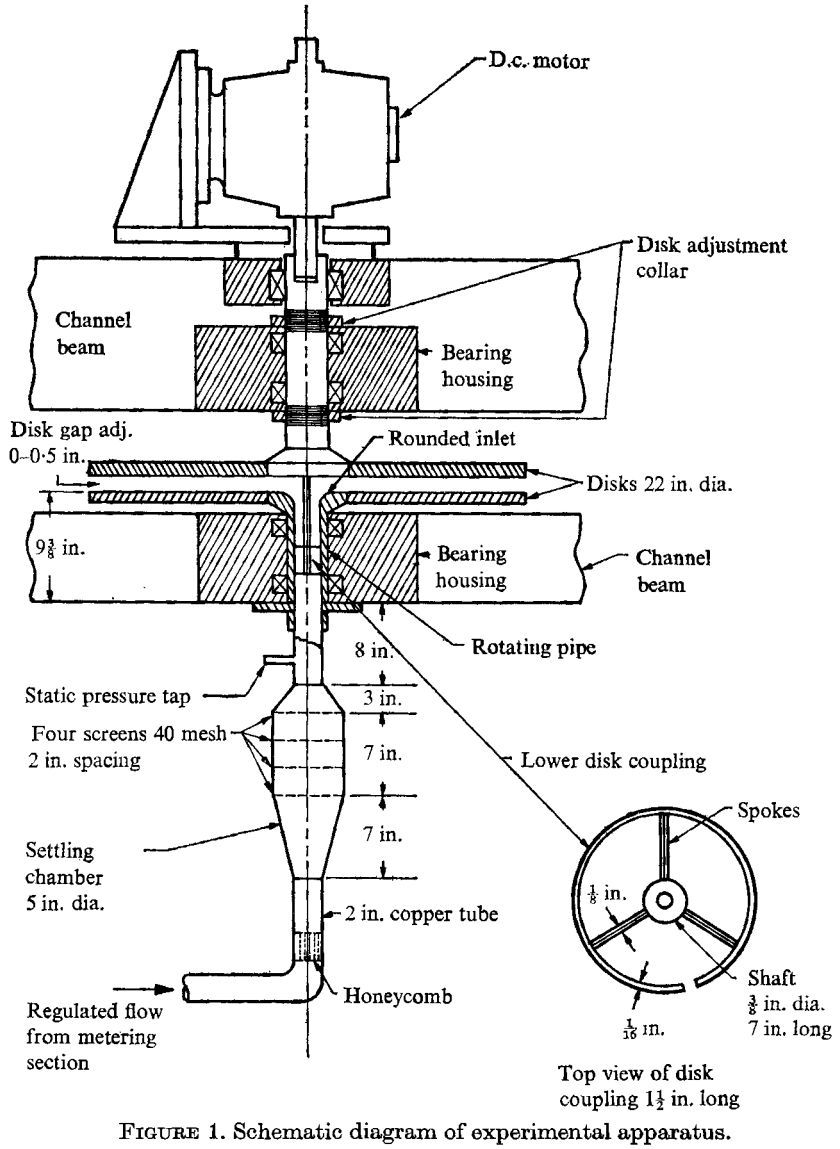

FIGURE 1. Schematic diagram of experimental apparatus.

muth (1967) with an upper frequency limit (– 3 db point) at 14 000 Hz. Turbulent components above 12 000 Hz were found to be insignificant under the flow conditions covered in the experiments. To obtain a true time-averaged velocity, the linearized voltage signal was integrated either by an integrating 'lag' amplifier, for small fluctuations, or by direct electronic integration, for larger fluctuations. A static-pressure probe was used to measure the radial pressure gradient between the disks. The probe could be moved radially and could be positioned parallel to the velocity vector at any radius.

After the rotational speed of the disks and the flow rate through the system had been set and the probe aligned properly so as not to be in its own wake, the velocity profile was measured. At any radial position 10–15 readings were taken

across one half of the disk gap. Smaller increments were used close to the disk surface, where the velocity gradient was greatest. The root-mean-square of the turbulent fluctuation, e.g. $(\overline{u^2})^{\frac{1}{2}}$, the radial component, was measured on a true r.m.s. voltmeter with a sufficiently large time constant to give a steady reading. Velocities as low as 2 ft/s could be measured to within $\pm 6\,\%$.

2.2. *Static pressure measurements*

The pressure transducer was always used to measure the static pressure in the test section since a fast pressure-reading response was necessary. The transducer amplifier was carefully zero adjusted before each run and the zero reading was rechecked afterwards. The pressure was measured relative to atmospheric pressure to an accuracy of $\pm 0{\cdot}001$ psi.

For pressure measurements between stationary disks the pressure probe was placed approximately in the middle of the disk gap in the traversing mechanism and aligned radially. When the disks were rotating great care had to be taken to obtain the true static pressure reading. If the probe was located parallel to the radius vector, some of the holes in the probe would sense a dynamic pressure since the total velocity vector is at an angle with the radial vector. To align the probe parallel to the velocity vector it was rotated about a vertical axis with the radial position of interest as its centre. By turning the probe until the pressure reading was a minimum, the direction parallel to the velocity vector was determined. The probe orientation parallel to the mean velocity vector was distinct and easy to find in practice.

3. Governing equations

3.1. *Momentum equations*

Representing each velocity component by a mean (denoted by an overbar) and a fluctuating part, i.e.,

$$U = \overline{U} + u, \quad V = \overline{V} + v, \quad W = \overline{W} + w,$$

in the co-ordinate system shown in figure 2 the turbulent flow between two disks is analysed under the following assumptions: (i) that gravity forces are negligibly small; (ii) that the mean flow is steady and incompressible; (iii) that the mean flow is axisymmetric; and (iv) that the average axial velocity component $\overline{W}$ is negligibly small compared with $\overline{U}$ and $\overline{V}$, the radial and tangential components, respectively. This condition prevails when the gap between the disks is small. In the system studied, the ratio of the disk spacing to the disk diameter was always less than 0·0136, satisfying the small-gap requirement. Introducing the above definitions and assumptions into the Navier–Stokes equations for a fixed co-ordinate system and using conventional averaging procedures yields the following momentum equations:

$$\overline{U}'\frac{\partial \overline{U}'}{\partial r'} - \frac{Re_T^2}{Re_Q^2}\frac{\overline{V}'^2}{r'} = -\frac{\partial \overline{P}'}{\partial r'} + \frac{2}{Re_Q}\frac{R}{h}\frac{\partial^2 \overline{U}'}{\partial z'^2} - \frac{\tilde{v}^2}{\overline{U}_{\mathrm{av}}^2}\frac{R}{h}\frac{\partial}{\partial z'}(\overline{u'w'}), \tag{1}$$

$$\overline{U}'\frac{\partial \overline{V}'}{\partial r'} + \frac{1}{r'}\overline{U}'\overline{V}' = \frac{2}{Re_Q}\frac{R}{h}\frac{\partial^2 \overline{V}'}{\partial z'^2} - \frac{\tilde{v}^2}{\overline{U}_{\mathrm{av}}\omega r}\frac{R}{h}\frac{\partial}{\partial z'}(\overline{v'w'}). \tag{2}$$

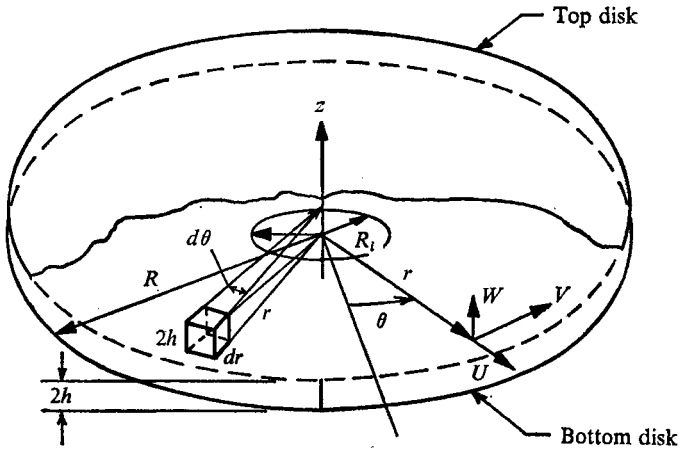

FIGURE 2. Cylindrical co-ordinate system.

These equations have been non-dimensionalized and scaled by two velocity scale factors $\overline{U}_{\mathrm{av}} = Q/4\pi rh$, where Q is the volumetric flow rate in ft^3/s, and ωr, where ω is the disk angular velocity in rad/s, for the radial and tangential velocity, respectively, by two length scales R and h for the horizontal and vertical distances, respectively, and by a pressure scale $\rho\overline{U}^2_{\mathrm{av}}$. The turbulent velocity scale for all three turbulent components is $\tilde{v}$. Two local Reynolds numbers, one related to the source flow and the other related to the rotational speed, result from the non-dimensionalization. The source-flow Reynolds number is

$$Re_Q = Q/2\pi r\nu = \overline{U}_{\mathrm{av}} \times 2h/\nu \tag{3}$$

and the rotational Reynolds number is

$$Re_T = 2\omega rh/\nu. \tag{4}$$

As will be shown later, the two Reynolds numbers defined by (3) and (4) actually describe important aspects of the flow.

The order-of-magnitude analysis indicates which parameters are significant. However, (1) and (2) have too many unknowns to be solved analytically and to obtain a solution one is forced to make an additional assumption.

3.2. *Integral momentum balance for rotating disks*

The radial pressure distribution is usually of most interest in practical applications. A simple force balance on an element of fluid with height equal to the disk spacing provides an expression for the radial pressure distribution if velocity profiles in the radial and tangential directions are known. The force balance for the element $dr \times r\,d\theta \times 2h$ in figure 2 is

$$\frac{\partial P}{\partial r} = \frac{\rho}{h}\int_0^h \frac{\overline{V}^2}{r}\,dz - \frac{\rho}{h}\frac{1}{r}\frac{\partial}{\partial r}\left[r\int_0^h \overline{U}^2\,dz\right] - \frac{\tau_R}{h}, \tag{5}$$

where τ_R is the shear stress at the disk surface. To solve this equation for the pressure, the radial and tangential velocity distributions must be known.

The radial velocity profile depends strongly upon the rotational Reynolds number and the profile cannot be expected to follow a universal law. However, for sufficiently high rotational Reynolds numbers the velocity profile in the tangential direction can be assumed to follow the $\frac{1}{7}$ power law

$$\overline{V} = \omega r[1-(1-K)(z/h)^{\frac{1}{7}}], \tag{6}$$

where K is the ratio of the centre-line tangential velocity to the disk surface velocity at radius r. K must be determined from experimental results and will depend on the source flow rate and rotational speed. In order to compute τ_0 an empirical relation such as that given by Schlichting (1968, p. 561),

$$C_f = \tau_0/\tfrac{1}{2}\rho\overline{U}^2 = 0{\cdot}079/Re^{\frac{1}{4}}, \tag{7}$$

may be used. This expression does not take rotational effects into account and the axial velocity $\overline{U}$ is defined for flow in ducts. Equation (7) must be modified to take the rotational effects into account if it is to be used to predict τ_0 in source flow between rotating disks. In place of $\overline{U}$, a total relative velocity with respect to the disks which takes the spiral motion into account could be used, for example. One such relative velocity is V_R given by

$$\overline{V}_R^2 = \overline{U}_{\mathrm{av}}^2 + (\omega r - \overline{V}_h)^2. \tag{8}$$

To use this expression the centre-line tangential velocity $\overline{V}_h$ must be measured or estimated.

In practice it is easier to define the relative velocity only in terms of disk surface speed and to replace $\overline{U}^2$ in (7) by the approximation

$$\overline{V}_R^2 = \overline{U}_{\mathrm{av}}^2 + \omega^2 r^2. \tag{9}$$

Since ω is known, the 'relative' velocity $\overline{V}_R$ may be computed directly. Replacing $\overline{U}^2$ with $\overline{V}_R^2$ in (7) we have

$$C_f = \tau_0/\tfrac{1}{2}\rho\overline{V}_R^2 = \alpha/Re_R^{\frac{1}{4}}, \tag{10}$$

where Re_R is the relative Reynolds number $\overline{V}_R 2h/\nu$ and α is a constant tc be determined from experimental data.

The shear stress τ_0 in (10) is the total shear stress at the disk surface and consists of radial and tangential components. If ϕ is the angle between the relative velocity and the radial vector, the shear stress τ_R in the radial direction becomes

$$\tau_R = \tau_0 \cos\phi = \tau_0(\overline{U}_{\mathrm{av}}/\overline{V}_R). \tag{11}$$

Using (10) in (11) gives

$$\tau_R = \tfrac{1}{2}\rho\overline{V}_R^2 \frac{\alpha}{Re_R^{\frac{1}{4}}} \frac{\overline{U}_{\mathrm{av}}}{\overline{V}_R} = \tfrac{1}{2}\rho\overline{U}_{\mathrm{av}}\overline{V}_R \frac{\alpha}{Re_R^{\frac{1}{4}}} \tag{12}$$

and the relative Reynolds number becomes

$$Re_R = \frac{\overline{V}_R 2h}{\nu} = \frac{(\overline{U}_{\mathrm{av}}^2 + \omega^2 r^2)^{\frac{1}{2}} 2h}{\nu} = \left[\left(\frac{\overline{U}_{\mathrm{av}} 2h}{\nu}\right)^2 + \left(\frac{\omega r 2h}{\nu}\right)^2\right]^{\frac{1}{2}}. \tag{13}$$

The relative Reynolds number may also be expressed as

$$Re_R = (Re_Q^2 + Re_T^2)^{\frac{1}{2}}. \tag{14}$$

After the radial and tangential velocity distributions have been integrated across the disk gap using the continuity equation and (6), equation (5) takes the form

$$\frac{dP}{dr} = \rho\left\{\frac{\omega^2}{8}(1+7K)\,r + \left(\frac{Q}{4\pi h}\right)^2 \frac{1}{r^3} - \frac{1}{2h}\frac{\alpha}{Re_R^{\frac{1}{4}}}\frac{Q\omega}{4\pi h}\left[\left(\frac{Q}{4\pi h\omega}\right)^2 \frac{1}{r^4}+1\right]^{\frac{1}{2}}\right\}. \tag{15}$$

For stationary disks ($\omega = 0$) integration of (15) gives

$$P_0 - \bar{P} = \frac{\rho}{2}\left(\frac{Q}{4\pi h}\right)^2\left[\left(\frac{1}{r^2}-\frac{1}{R^2}\right) - \frac{1}{h}\frac{\alpha}{Re_Q^{\frac{1}{4}}}\left(\frac{1}{r}-\frac{1}{R}\right)\right]. \tag{16}$$

For co-rotating disks, however, (15) must be integrated numerically because the shear stress term cannot be integrated analytically. Details of the integration are presented by Bakke (1969).

4. Experimental results

4.1. *The flow field between two stationary disks*

Velocity profiles were measured with disk spacings $h/R = 0{\cdot}00909$ ($2h = 0{\cdot}2$ in.) and $h/R = 0{\cdot}01363$ ($2h = 0{\cdot}3$ in.). The smallest disk spacing at which measurements could be taken was determined by the size of the hot-wire probe with which the velocity traverses were made.

Case 1. $h/R = 0{\cdot}00909$ ($2h = 0{\cdot}2$ in.). Figure 3 shows the dimensionless mean radial velocity profiles and turbulent intensities as a function of the dimensionless vertical distance z/h at four different radial positions in the test section for two different source flow rates.

In figure 3(*a*) the radial velocity profiles at four different radial positions and at a lower source flow rate are compared with the creeping-flow solution

$$\bar{U}/\bar{U}_h = 2(z/h)\,(1-z/2h).$$

The velocity profiles closely approach a parabolic distribution with increasing radius. This may appear to indicate that the flow is laminar, and Moller (1963) suggested that the approach of the mean velocity profile to a parabolic shape is a valid indication of laminar flow. Figure 3(*b*) shows, however, that the turbulent intensity is increasing with increasing radius, and one must therefore conclude that the flow has not become laminar although the mean velocity profiles have approached a quasi-parabolic velocity distribution. Detailed results of these transition phenomena are given by Bakke & Kreith (1969).

Some of the mean velocity profiles shown in figure 3(*a*) have inflexion points close to the disk surface. The inflexion point in the radial velocity profiles is caused by the adverse pressure gradient which results from the radial deceleration of the flow. However, measurements were difficult to make in the region where the velocity profiles are inflected since the thermal interaction between the hot wire and the disk surface results in false signals in this region.

The relative turbulence level $(\overline{u^2})/\bar{U}_h$ has a maximum close to the surface as shown in figure 3(*b*). As the flow moves outwards through the test section the maximum turbulence level occurs at a greater distance from the surface; this is

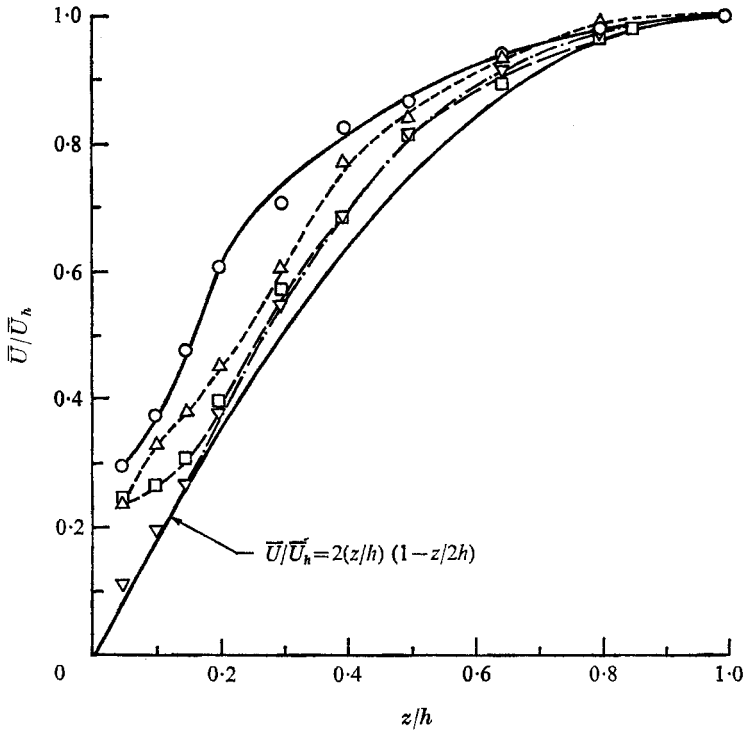

(*a*)

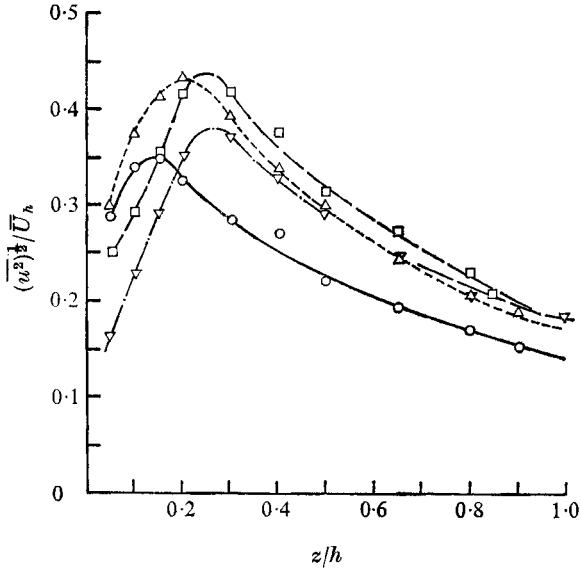

(*b*)

FIGURE 3. For legend see facing page.

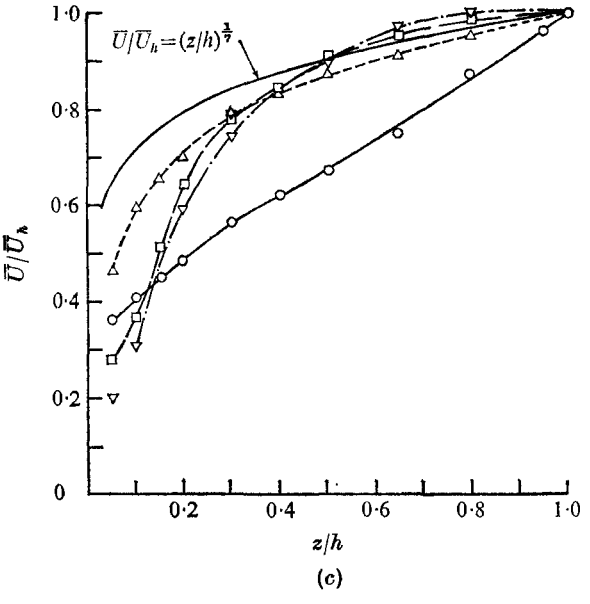

FIGURE 3. (*a*) Mean radial velocity $\overline{U}/\overline{U}_h$ *vs.* vertical distance z/h at four radial positions for a source flow rate $Q = 0{\cdot}638\,\text{ft}^3/\text{s}$. (*b*) Relative turbulence intensity profile at $Q = 0{\cdot}638\,\text{ft}^3/\text{s}$. (*c*) Radial velocity for $Q = 1{\cdot}43\,\text{ft}^3/\text{s}$. Rotation rate $N = 0$; $h/r = 0{\cdot}0091$.

		–·–·–, ▽	– – –, □	------, △	———, ○
(*a*), (*b*)	r/R	0·955	0·863	0·773	0·545
	Re_Q	592	654	731	1036
(*c*)	r/R	0·955	0·773	0·545	0·318
	Re_Q	1328	1640	2322	3980

not unexpected since the Reynolds number decreases with increasing radius and consequently the laminar sublayer thickens with increasing radius. The point of maximum relative turbulence intensity indicates the point of maximum turbulence production and it occurs just above the disk surface, where viscous forces dominate.

In figure 3(*c*) velocity profiles at a high source-flow Reynolds number are compared with the $\frac{1}{7}$ power law profile.

Case 2. $h/R = 0{\cdot}01363$ ($2h = 0{\cdot}3$ in.). As the gap between the disks was increased the inlet velocity profiles became less symmetric since, with increasing disk spacing, the separated region at the lower disk became larger. As a result the mean radial velocity profiles for a 0·3 in. disk spacing did not approach the parabolic profile as rapidly as the profiles with a 0·2 in. disk spacing. The separation at the inlet with a 0·3 in. disk spacing was more extensive and produced a flow with a higher turbulence level throughout the test section.

4.2. *The flow field between two co-rotating disks*

The flow between two co-rotating disks with source flow was investigated for the same two disk gaps as for the irrotational study, namely $h/R = 0{\cdot}00909$ and $h/R = 0{\cdot}01363$. The disk spacings were made the same so that the influence of the centrifugal forces on the flow could be studied by direct comparison.

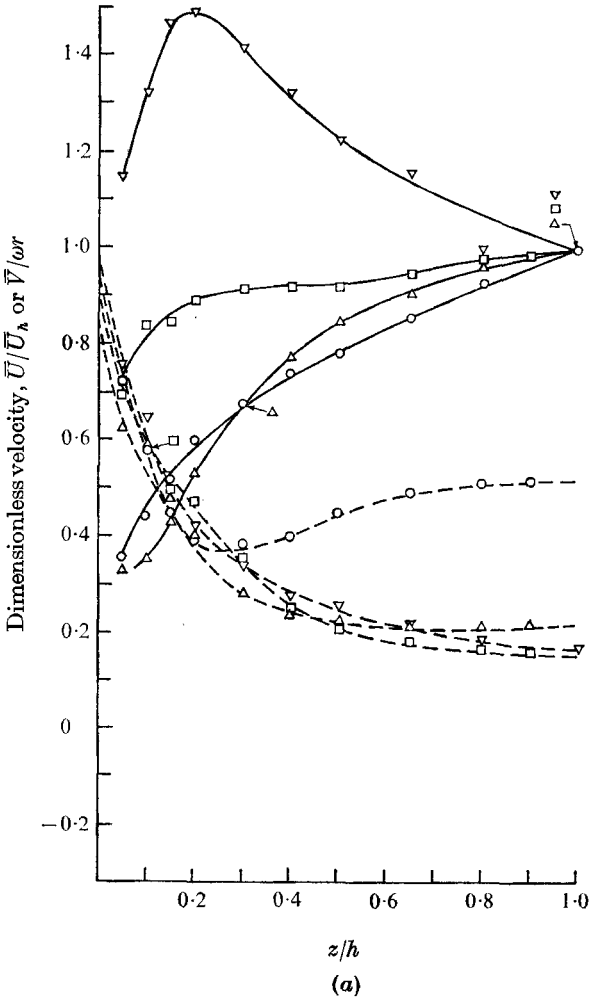

FIGURE 4. For legend see facing page.

Case 1. $h/R = 0{\cdot}00909$ ($2h = 0{\cdot}2$ in.). Figures 4 and 5 show mean radial and tangential velocity profiles for several flow conditions at different radii. The data cover a range of source-flow Reynolds numbers $Q/2\pi r\nu$ from 592 to 3980 and rotational Reynolds numbers $2\omega r h/\nu$ from 1300 to 11680. The shape of the profiles depends on both the flow and rotational Reynolds numbers.

A certain distance from the inlet of the test section is needed for the flow to develop a symmetric profile across the disk gap in both the radial and tangential directions. As the rotational speed is increased this entrance length decreases. The disks supply momentum to the fluid near the disk through viscous shear and since the centrifugal forces near the disk become larger with increasing radius the radial velocity profile develops a maximum near the disk for sufficiently large rotational rates. At one radial position for each value of $Re_T - Re_Q$ the radial velocity is approximately uniform across the disk gap; at all points downstream of this radius a maximum in the radial velocity profile develops close to the disk.

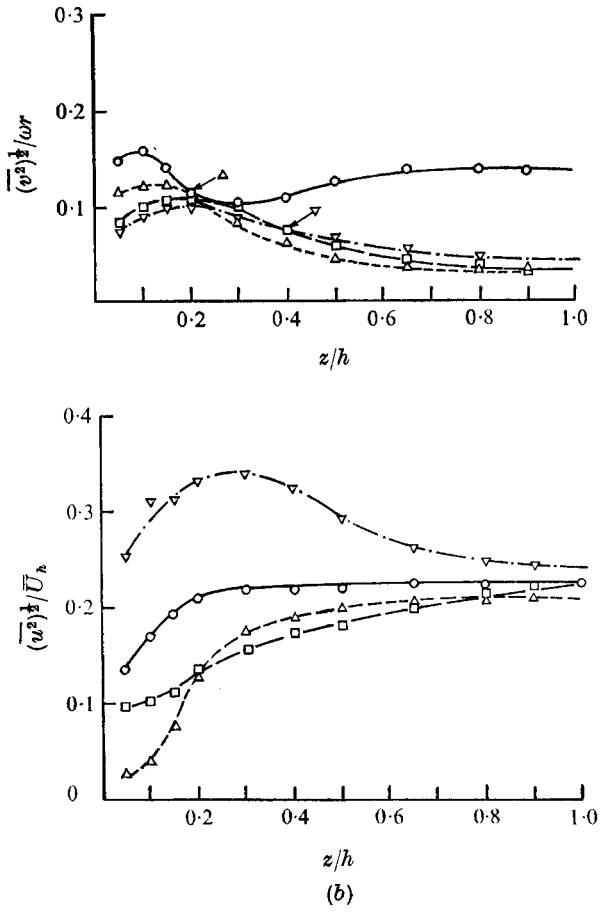

FIGURE 4. (*a*) Radial (solid lines) and tangential (broken lines) mean velocity profiles and (*b*) turbulence intensity profile. $h/R = 0{\cdot}0091$, $Q = 0{\cdot}638\,\mathrm{ft^3/s}$, $N = 500\,\mathrm{r.p.m.}$

	▽	□	△	○
r/R	0·955	0·773	0·545	0·318
Re_Q	592	654	731	1036
Re_T	3902	3160	2230	1301

This is illustrated in figure 5, where the dimensionless radial velocity $\overline{U}/\overline{U}_h$ is plotted against the dimensionless vertical distance z/h, at four radial positions.

The dimensionless momentum equations developed in § 3.1 illustrate the significance of the two Reynolds numbers. The viscous term in (1) is large close to the disk surface, where the radial velocity gradient $\partial^2 U/\partial z^2$ is large. With increasing rotational speed the coefficient Re_T^2/Re_Q^2 in (1) becomes significant. In the region where the viscous and Reynolds stress terms in (1) are both small, i.e. for the central core between the two disks, the size of the coefficient of the centrifugal force term Re_T^2/Re_Q^2 will determine the influence of the centrifugal forces on the flow field. The ratio Re_T^2/Re_Q^2 is simply the ratio of the square of two velocities, i.e. $(\omega r/\overline{U}_{\mathrm{av}})^2$.

Another parameter of significance is formed by multiplying Re_T/Re_Q by r/R.

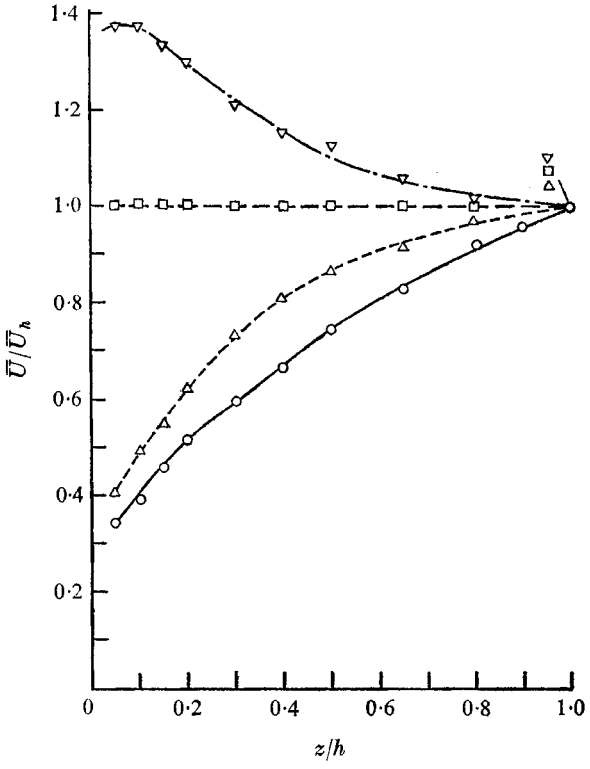

FIGURE 5. Radial mean velocity profiles at $Q = 1{\cdot}43\,\mathrm{ft}^3/\mathrm{s}$ and $N = 1493$ r.p.m.; $h/R = 0{\cdot}0091$.

	—·—, ▽	——, □	– – –, △	——, ○
r/R	0·955	0·773	0·545	0·318
Re_Q	1328	1640	2322	3980
Re_T	11680	9444	6676	3894

This parameter, X, which, as shown below, predicts when centrifugal forces dominate, is defined as

$$X = \frac{Re_T}{Re_Q}\frac{r}{R} = \frac{\omega r}{\overline{U}_{\mathrm{av}}}\frac{r}{R}. \tag{17}$$

The radial pressure distribution has a point of inflexion at the radial position at which the radial velocity distribution is uniform across most of the disk gap ($r/R = 0{\cdot}773$). The same correspondence was found with a 0·3 in. disk gap. At this point the viscous forces and Reynolds stresses, which tend to maintain the velocity gradient, are balanced against the centrifugal forces, which are strong close to the rotating disk surfaces. The resulting velocity profile has a very large velocity gradient in a small region very close to the surface and a constant radial velocity over the remainder (approximately 95 %) of the gap. The parameter X was calculated from the experimental data shown in figure 5 at the radial position where $\overline{U}$ was approximately constant across the gap and was found to be approximately 4·0. For greater radial distances the centrifugal forces become dominant and the profiles show a characteristic maximum velocity near the rotating disk surface. This behaviour is clearly shown in figure 5 for $r/R = 0{\cdot}955$.

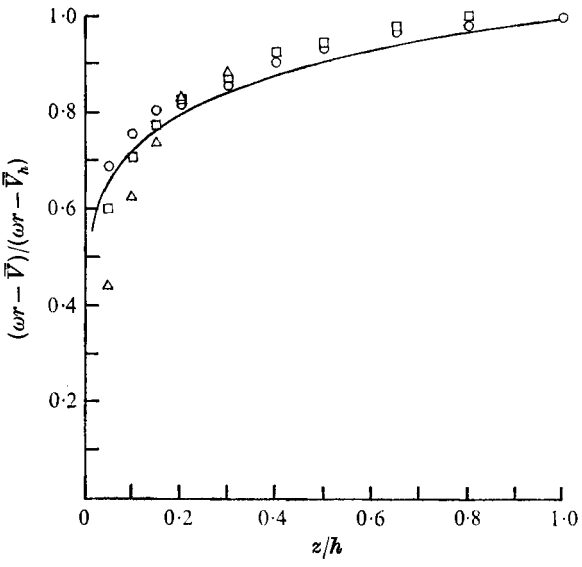

FIGURE 6. Comparison between measured mean tangential velocity profiles and the '$\frac{1}{7}$ power law' distribution. $h/r = 0{\cdot}0091$, $r/R = 0{\cdot}955$. △, $Re_Q = 128$, $Re_T = 11680$; □, $Re_Q = 1328$, $Re_T = 5840$; ○, $Re_Q = 891$, $Re_T = 5840$; ——, $(\omega r - \bar{V})/(\omega r - \bar{V}_h) = (z/h)^{\frac{1}{7}}$.

The pressure distribution points of inflexion for all runs were found to fall within the region $3{\cdot}7 < X < 4{\cdot}8$. Whenever X is greater than 3·7, the radial velocity distribution changes from a profile with a continuously increasing velocity to a distribution with a maximum close to the disk surface.

The relationship between the radial velocity, the source flow rate and the disk rotation is complex. Since the mean radial velocity profile depends on the radial position, the source flow and the rotational speed of the disks, no universal turbulent velocity distribution law can be expected to apply. One might, however, expect the tangential velocity profile to approach a 'universal' law at sufficiently high rotational Reynolds numbers since the influence of the asymmetrical inlet conditions diminishes rapidly as the rotational speed increases. This prediction was verified by plotting the relative velocity ratio $(\omega r - \bar{V})/(\omega r - \bar{V}_h)$ *vs.* z/h at a radial position $r/R = 0{\cdot}955$. As shown in figure 6 the profiles deviate somewhat from the $\frac{1}{7}$ power law at small vertical distances; however, the data fit a $\frac{1}{7}$ power law reasonably well even at the smallest source-flow Reynolds number.

K, the ratio of the centre-line tangential velocity $\bar{V}_h$ to the disk velocity ωr, was determined experimentally. Plotting K *vs.* X showed that the flow parameter X is significant since a single curve correlates all the data in figure 7. The value for K varies considerably with flow conditions and radial distance. At the inlet to the test section the mean tangential velocity is small and does not differ much from the disk velocity. This can be seen in figure 4(*a*) ($r/R = 0{\cdot}318$), where $K = 0{\cdot}5$; at $r/R = 0{\cdot}545$, however, K has dropped to 0·2. Figure 7 shows that K reaches a minimum value of about 0·12 for X between 2 and 3. For X equal to 4, the centrifugal forces become dominant and K increases for X larger than four.

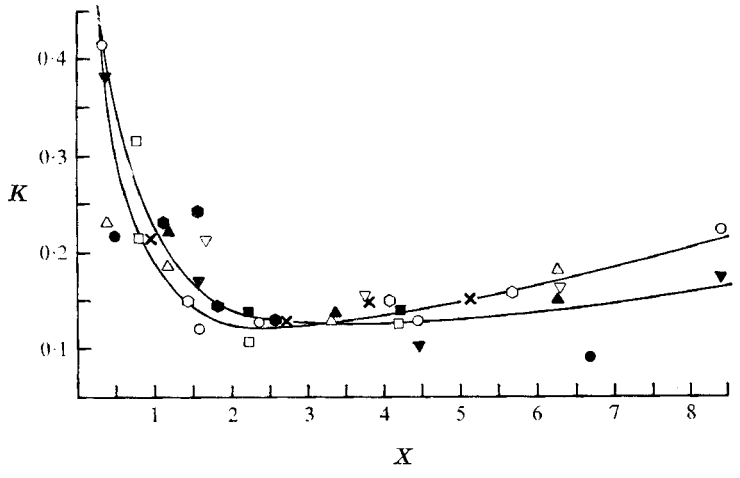

FIGURE 7. Measured core rotation parameter K *vs.* flow parameter X for two disk spacings.

$h/R = 0{\cdot}0136$

▲	■	▼	●	⬢
$Q = 0{\cdot}96\,\text{ft}^3/\text{s}$	$Q = 1{\cdot}43\,\text{ft}^3/\text{s}$	$Re_Q = 2322$	$Q = 1{\cdot}43\,\text{ft}^3/\text{s}$	$Re_Q = 976$
$N = 500$ r.p.m.	$N = 500$ r.p.m.	$Re_T = 6676$	$N = 1500$ r.p.m.	$Re_T = 3265$

$h/R = 0{\cdot}0091$

	○	□	△	▽	×	⬡
Q (ft³/s)	1·43	1·43	0·96	0·64	1·56	1·56
N (r.p.m.)	1493	747	500	1000	1993	

The relative turbulence intensity $(\overline{u^2})^{\frac{1}{2}}/\overline{U}$ increases with increasing radius. A positive pressure gradient promotes turbulence and some of the energy supplied by the rotating disks is converted into turbulence. Turbulence data and a detailed discussion of the energy conversion are given by Bakke (1969).

Case 2. $h/R = 0{\cdot}0136$ ($2h = 0{\cdot}3$ in.). As in case 1, the radius at which the inflexion point in the pressure distribution occurs was found to correspond to the radius where the radial velocity component across the gap was approximately constant. The values of X which correspond to the position at which the radial velocity is constant were found to be the same in a 0·3 in. gap as in a 0·2 in. gap.

The K *vs.* X plot for the 0·3 in. disk gap (figure 7) is similar to that for the 0·2 in. gap. However, for a 0·3 in. gap K does not increase beyond the minimum point as rapidly as for a 0·2 in. gap since for the larger disk spacing the influence of the centrifugal forces near the centre of the gap is smaller for the greater spacing.

4.3. *Comparison of the flow between two rotating and two stationary parallel disks with source flow*

The effect of centrifugal forces on the flow may be seen by comparing mean velocities, turbulent intensities and radial pressure distributions for the same source flow rate through the test section with and without disk rotation.

Figures 3(*a*) and 4(*a*), respectively, show the velocity profiles at a source flow rate of $Q = 0{\cdot}638\,\text{ft}^3/\text{s}$ for stationary disks and for disks rotating at 500 r.p.m.

with 0·2 in. disk spacing. At $r/R > 0{\cdot}863$ the mean radial velocity profiles without rotation approach the creeping-flow solution, but when the disks are rotating, the mean radial velocity profiles develop a maximum near the disk surface.

The radial velocity profile shown in figure 4(*a*) has an inflexion point at $r/R = 0{\cdot}545$. Figure 3(*a*) shows that the corresponding radial velocity profile without rotation also has an inflexion point at the same radial position. This indicates the instability of the flow due to the adverse pressure gradient. In figure 4(*a*), however, the inflexion point has disappeared at $r/R = 0{\cdot}773$, indicating that the centrifugal forces in the region close to the rotating disks are sufficiently strong to stabilize the flow.

The stabilization of the flow by the centrifugal forces can also be seen by comparing the turbulent intensity profiles for the stationary and rotating cases. Without rotation (figure 3*b*) the relative turbulence intensity is greatest at $r/R = 0{\cdot}773$ and the maximum in the turbulence distribution profile lies at $z/h = 0{\cdot}2$, approximately at the inflexion point of the mean radial velocity profile. At this vertical position the relative turbulence intensity is about 0·45 whereas with rotation, as shown in figure 4(*b*), the characteristic peak disappears and the turbulence level is considerably reduced.

The radial pressure distributions in flow between stationary and rotating disks are shown in figure 8; in flow between stationary disks the pressure increases smoothly towards the disk rim, but when the disks are rotating the centrifugal forces cause a rapid increase in the pressure distribution curve near the disk rim. As the disk speed is increased further, the radial pressure distribution develops an inflexion point and a rapid pressure increase occurs near the disk rim.

4.4. *Similarity of the velocity profiles*

Because of the large variation in the pressure gradient through the test section complete similarity cannot be expected in the sense that all velocity profiles can be condensed into a single curve characterized by a dimensionless parameter for the entire range of radial positions. However, it is possible that similar profiles for a smaller range of radial positions could be established. In source flow between stationary disks the flow Reynolds number $Q/2\pi r\nu$ is the similarity parameter. For rotating disks two Reynolds numbers have been defined – one involving the source flow rate, the other involving the rotation – which might serve as similarity parameters. By making velocity traverses across the disk gap at different radial positions with the same flow and rotational Reynolds numbers the proposed similarity parameters could be checked. From the experiments it was apparent that the rotational Reynolds number based upon the Coriolis force ($\omega r^2/\nu$) proposed by some investigators did not give similar velocity profiles at different radial positions. The rotational Reynolds number Re_T, however, was found to be the correct similarity parameter. Some of the results of the measurements are shown in figures 9(*a*) and (*b*), where the dimensionless velocities $\overline{U}/\overline{U}_{av}$ and $\overline{V}/\omega r$ are plotted against the dimensionless vertical distance z/h.

The static pressure at each radial position was also measured and the dimensionless pressure difference $(P_0 - \overline{P})/P_0$ was plotted *vs.* r/R. It was found that, when the dimensionless pressure gradient, the source flow and the rotational Reynolds

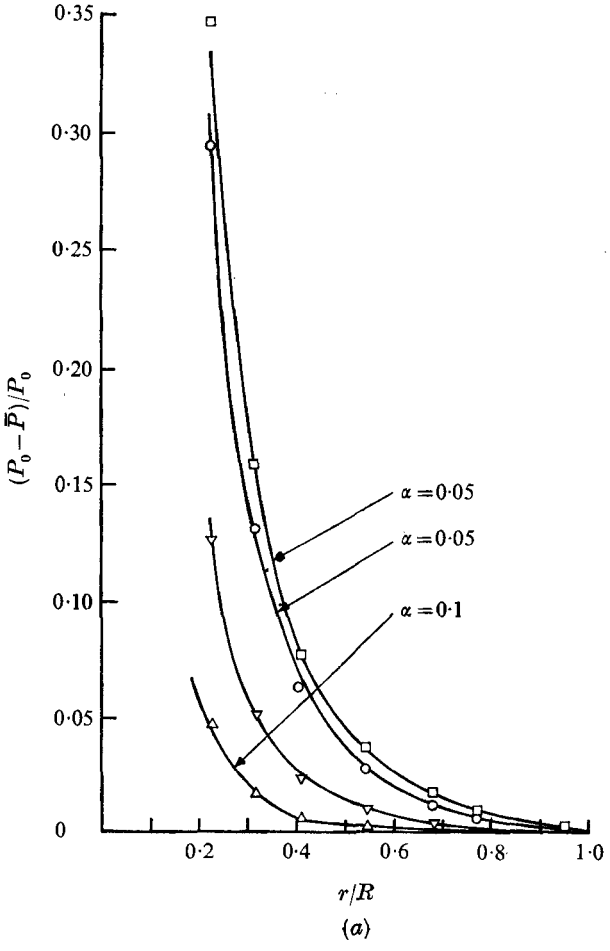

FIGURE 8. For legend see facing page.

number had the same value at any radial position, the velocity profiles were similar. This is shown in figure 9 (*a*), where the dimensionless velocity profiles for $Re_Q = 1602$ and $Re_T = 3265$ are plotted for a disk gap of 0·3 in. Figure 9 (*b*) shows the velocity profiles at the same flow Reynolds number as those in figure 9 (*a*), but with a rotational Reynolds number $Re_T = 11063$. These profiles have a maximum radial velocity close to the disk surface. The profiles in figure 9 (*b*) are similar at the two larger radial positions, but the lack of similarity at $r/R = 0{\cdot}545$ could be anticipated from the pressure distribution. The pressure gradient at $r/R = 0{\cdot}545$ is much larger than at $r/R = 0{\cdot}773$ and at $r/R = 0{\cdot}864$. However, the pressure gradients at the two larger radial positions are equal and tangential velocity profiles are also similar at these two radii. Whenever similarity was found in the radial velocity profiles, similarity also existed in the tangential and total velocity profiles.

Several checks for similarity were also made with a disk gap of 0·2 in. Similarity was found to exist both in the radial as well as the tangential directions. Although for Reynolds numbers identical to those for a 0·3 in. disk spacing the radial pro-

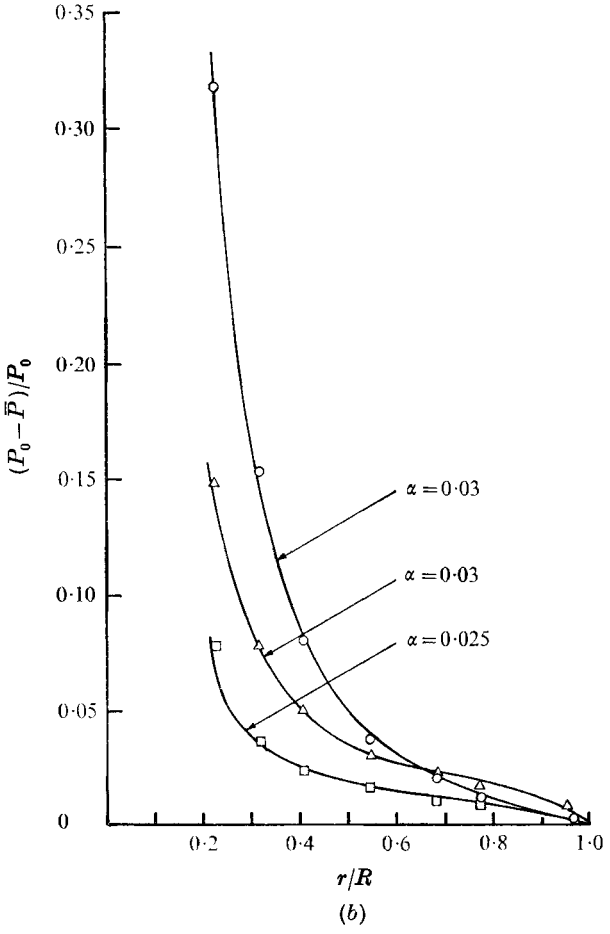

FIGURE 8. Comparison of calculated and measured radial pressure distributions for (*a*) stationary disks ($N = 0$) and (*b*) small rotational speeds and source flow rates. $h/R = 0{\cdot}0091$.

		△	▽	○	□
(*a*)	Q (ft³/s)	0·638	0·96	1·43	1·56
(*b*)	Q (ft³/s)	0·961	—	1·43	0·638
	N (r.p.m.)	747	—	500	500

files for both gaps have the same general shape, they are not strictly similar. Since the pressure gradient is inversely proportional to the disk spacing [see equation (15)], the pressure gradient is larger with the 0·2 in. disk spacing than with the 0·3 in. gap. Hence, the velocity profiles cannot be expected to be similar for different disk spacings even though the two Reynolds numbers are the same.

Similarity conditions were also investigated for stationary disks, where the source-flow Reynolds number $Q/2\pi r\nu$ is the similarity parameter. It was found that, when the pressure gradient was the same at different radial positions, the profiles were similar for given values of the source-flow Reynolds number.

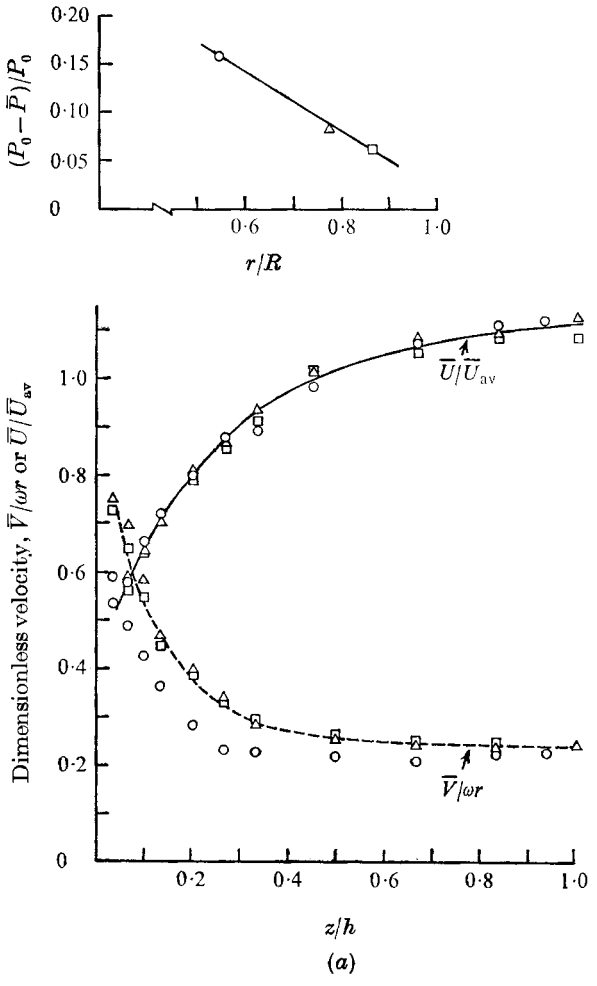

FIGURE 9. For legend see facing page.

5. Discussion of experimental and analytical results

5.1. *Source flow between two stationary disks*

To carry out the integration resulting in (16) (for $\omega = 0$) a value for the constant α in the friction coefficient must be assumed. According to (7), α is 0·079, but this value is based upon the assumption that a $\frac{1}{7}$ power velocity distribution exists. Since it was shown earlier that the radial velocity profiles do not follow the $\frac{1}{7}$ power distribution, the actual value for α would be expected to differ from that in the Blasius formula. Several values for α were substituted in the equation and the calculated pressure distributions were compared with the measured distributions.

Some calculated and measured pressure distributions for a 0·2 in. disk gap are shown in figure 8(*a*), where the dimensionless pressure $(P_0-\bar{P})/P_0$ is plotted against the dimensionless radial distance r/R. With an appropriate average value for α the agreement between the calculated and measured distributions is close.

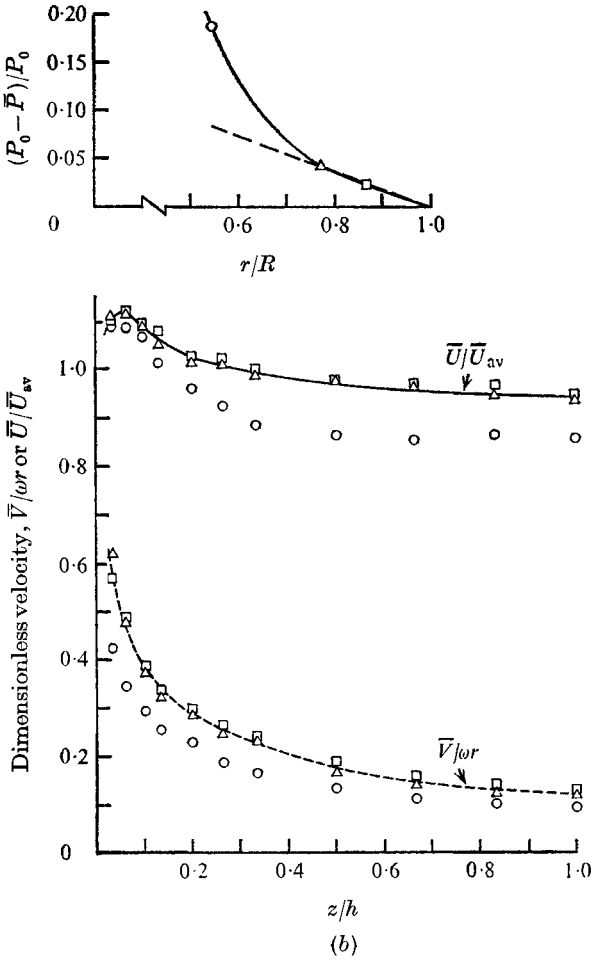

FIGURE 9. Similarity of pressure gradient, radial mean velocity and tangential mean velocity profiles for $Re_Q = 1602$ and $h/R = 0{\cdot}0136$. (*a*) $Re_T = 3265$. (*b*) $Re_T = 11063$. ○, $r/R = 0{\cdot}545$; △, $r/R = 0{\cdot}773$; □, $r/R = 0{\cdot}864$.

This indicates that (16) is a useful expression for the irrotational pressure distribution when the 'best fit' average value for α is known.

To determine the proper value of α to use in (16), the pressure profile was computed from (16) with several assumed values of α for several source flow rates and afterwards compared with the experimental profile for each flow rate. The 'best fit' value of α was determined in this manner. It was found that these values could be correlated with the source-flow Reynolds number evaluated at the disk rim ($r = R$). A regressive analysis of α *vs.* $Re_{Q,R}$ gave the linear relation

$$\alpha = 0{\cdot}1345 - 0{\cdot}0000609 Re_{Q,R} \tag{18}$$

in the range $400 < Re_{Q,R} < 1400$. Since Hasinger & Kehrt (1963) showed that the flow may not be laminar at source-flow Reynolds numbers as low as 237, not even at such small values of Re_Q should a friction factor independent of Re_Q be used to calculate the radial pressure distribution.

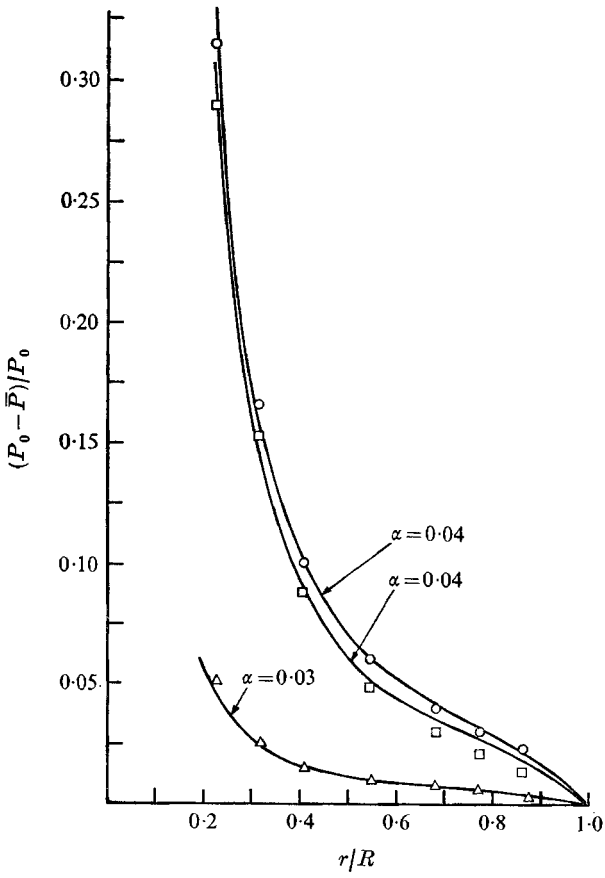

FIGURE 10. Comparison of calculated and measured radial pressure distributions for co-rotating disks; $h/R = 0{\cdot}01136$. ○, $Q = 1{\cdot}56\,\text{ft}^3/\text{s}$, $N = 1000$ r.p.m.; □, $Q = 1{\cdot}56\,\text{ft}^3/\text{s}$, $N = 800$ r.p.m.; △, $Q = 0{\cdot}638\,\text{ft}^3/\text{s}$, $N = 400$ r.p.m.

5.2. *Source flow between two co-rotating disks*

The radial pressure distribution in the test section with co-rotating disks was calculated by integrating (5) numerically. To carry out this integration, values for K had to be assumed and the relationship between K and X shown in figure 7 programmed into the integration routine.

Radial pressure distributions were measured with disk spacings of 0·2 in., 0·25 in. and 0·3 in. The results for a disk spacing $h/R = 0{\cdot}01136$ ($2h = 0{\cdot}25$ in.) are shown in figure 10, where the dimensionless pressure $(P_0-\bar{P})/P_0$ is plotted against the dimensionless radial distance r/R. The distributions calculated using (5) with the 'best fit' values of α are also shown. The best value of α for use in (5) was determined from the measured pressure distribution by a method analogous to that used for the irrotational case. It was found that α was a function of the source flow rate and the disk speed. The values for α from these calculations are scattered in a band from 0·025 to 0·04 but no simple functional relationship among α, Re_Q and Re_T was found.

The velocity gradients were calculated from the assumed friction-coefficient expressions and the calculated gradients were compared with the experimental data. The initial slope of the measured velocity profiles was not used because reliable hot-wire measurements could not be made near the surface.

For rotational speeds below 800 r.p.m., the agreement between the calculated and measured pressure distributions was good. However, as the ratio between the rotational and source-flow Reynolds numbers became greater, the measured and calculated distributions diverged. For example, for a source flow rate of 1·43 ft^3/s and a disk speed N of 747 r.p.m. the agreement between calculated and measured distributions is good, whereas for $Q = 1{\cdot}43$ ft^3/s and $N = 1493$ r.p.m. the agreement is less satisfactory.

The parameter X defined by (17) predicts the conditions under which the centrifugal forces dominate. For X larger than 4 an inflexion point appears in the measured pressure distribution. The pressure distribution analysis of §3.2 is, therefore, only applicable up to $X = 4$. At larger values of X the measured and calculated pressure distributions diverge. It is felt that this divergence is caused by a stalling effect in the flow system. For large values of X it was found that the low pressure at the inlet to the test section caused some inflow to occur and under these conditions the assumptions on which the analysis is based are invalid.

6. Conclusions

In source flow between two parallel stationary disks the flow decelerates because of the increasing flow area and is consequently subjected to an adverse pressure gradient. As the fluid moves radially outwards the flow Reynolds number decreases and the velocity profiles between the disks were found to approach a quasi-parabolic profile. However, the profiles exhibited inflexion points close to the disk surfaces and the turbulence level did not decrease substantially after the velocity profiles had approached a parabolic shape.

An analysis of the radial pressure measurements showed that for small disk gaps (0.2 in. or less) the friction factor was approximately the same as for flow in a rectangular duct. When the disk gap was increased to 0·3 in., however, the separated region near the inlet was larger and the friction factor used in the analysis had to be reduced to obtain agreement between the calculated and the measured radial pressure distributions.

For the case of co-rotating disks, similarity parameters were determined by non-dimensionalizing the momentum equations. Two parameters appeared: a source-flow Reynolds number $Q/2\pi r\nu$ and a rotational Reynolds number $2\omega rh/\nu$. The sufficiency of these two parameters to describe similarity was verified by making velocity traverses at different radial positions for the same source-flow and rotational Reynolds numbers. At moderate rotations ($N < 800$ r.p.m.) the radial as well as the tangential profiles were found to be similar provided that the pressure gradient was the same at each radial position.

An analysis of the dimensionless momentum equations also showed that in the flow field outside the boundary layer the centrifugal force becomes strong when

the rotational Reynolds number is sufficiently large, i.e. when the term in (1) with the coefficient Re_T^2/Re_Q^2 becomes significant. A local flow parameter

$$X = rRe_T/Re_Q R$$

was defined. It was found that for values of X of approximately 4 the centrifugal forces were sufficiently strong to produce an essentially uniform radial velocity across the centre of the disk gap. However, for $X > 4$ a maximum in the velocity profile exists close to the rotating disk surface. The flow parameter X has therefore been shown to be useful in the prediction of flow conditions under which the centrifugal forces dominate the central region. It was also found that a uniform radial velocity across the centre of the disk gap was associated with an inflexion point in the radial pressure distribution.

It was found that for sufficiently high rotational speeds and at radial positions sufficiently removed from the source the effects of the asymmetrical inlet conditions disappeared and the agreement between the $\frac{1}{7}$ power velocity distribution and the measured tangential velocity profiles was good. The ratio of the centre-line tangential velocity to the disk velocity was found to vary with radial position and the flow parameter X. The ratio was found to be large for very small values of X, to decrease with increasing X, and then to increase with X again as the centrifugal forces became dominant. The variation of the centre-line to disk velocity ratio K was also found to depend on the disk spacing.

Velocity and turbulence intensity profiles in source flow between two stationary and two co-rotating disks were used to study the effect of the centrifugal forces on the flow. It was found that the centrifugal forces tend to stabilize the flow. Owing to this stabilizing effect, which increases with disk speed, the inflexion points in the velocity profiles, present at low rotational speed, disappeared at higher speed and the turbulence intensity simultaneously diminished. As the disk velocity was increased further, however, the turbulence intensity increased again owing to the increasing shearing force between the disks and the fluid.

A friction factor for calculating the radial pressure distribution in source flow between two rotating disks was developed empirically and the agreement between the analysis and measurements was found to be good for moderate speeds ($N < 800$ r.p.m.). For values of X greater than 4 the theory and the data diverge owing to a stalling effect in the flow.

The authors of this paper gratefully acknowledge helpful discussions with Professor D. Kennedy in the course of this research and the financial assistance of the National Science Foundation.

REFERENCES

Adams, R. & Rice, W. 1970 Experimental investigation of the flow between co-rotating disks. *J. Appl. Mech.* **92**, 844–849.

Bakke, E. 1969 A theoretical and experimental investigation of the flow phenomena between two co-rotating parallel disks with source flow. Ph.D. thesis, University of Colorado.

Bakke, E. & Kreith, F. 1969 Inverse transition in radial diffusers. *A.S.M.E.–A.I.Ch.E. Heat Transfer Conf. Minneapolis; A.S.M.E. Paper*, no. 69-HT-33.

BERGER, E., FREYMUTH, P. & FROBEL, E. 1963 Use of feedback control in the development of a constant-temperature hot-wire anemometer. *Boeing Sci. Res. Lab. Trans.* no. 198.

BREITER, M. C. & POHLHAUSEN, K. 1962 Laminar flow between two parallel rotating disks. *Aero. Res. Lab. Wright-Patterson AFB, Ohio Rep.* ARL62-318.

DAILY, J. W., ERNST, W. D. & ASBEDIAN, V. V. 1964 Enclosed rotating disks with superimposed throughflow. *Hydrodyn. Lab. Rep. Dept. Civil Engng, M.I.T.* no. 64.

DAILY, J. W. & NECE, R. E. 1960 Chamber dimension effects on induced flow and frictional resistance of enclosed rotating disks. *J. Basic Engng, Trans. A.S.M.E.* **82**, 217–232.

DORFMAN, L. A. 1963 *Hydrodynamic Resistance and the Heat Loss of Rotating Solids.* (trans. N. Kemmer). Oliver & Boyd.

FREYMUTH, P. 1967 Feedback control theory for constant-temperature hot-wire anemometers. *Rev. Sci. Instrum.* **38**, 677–681.

GREENSPAN, H. P. 1968 *The Theory of Rotating Fluids.* Cambridge University Press.

HAGIWARA, T. 1962 Studies on the characteristics of radial-flow nozzles. *Bull. A.S.M.E.*, **5** (20), 656–683.

HASINGER, S. H. & KEHRT, L. G. 1963 Investigation of a shear-force pump. *J. Engng for Power*, **85**, 201–207.

KREITH, F. 1968 Convection heat transfer in rotating systems. *Adv. Heat Transfer*, **5**, 129–251.

KREITH, F., DOUGHMAN, E. & KOZLOWSKI, H. 1963 Mass and heat transfer from an enclosed rotating disk with and without source flow. *J. Heat Transfer*, **85**, 153–163.

LICHT, L. & FULLER, D. C. 1954 A preliminary investigation of an air lubricated hydrostatic thrust bearing. *A.S.M.E. Paper*, 54-LUB-18.

LIVESEY, J. L. 1960 Inertia effects in viscous flow. *Int. J. Mech. Sci.* **1**, 84.

MATSCH, L. A. & RICE, W. 1968 An asymptotic solution for laminar flow of an incompressible fluid between rotating disks, *J. Appl. Mech.* **90**, 155–159.

MOLLER, P. S. 1963 Radial flow without swirl between parallel disks. *Aero. Quart.* **24**, 163–186.

OSTERLE, J. F., CHOU, Y. T & SAIBEL, E. A. 1957 The effects of lubricant inertia in journal bearing lubrication. *J. Appl. Mech.* **24**, 494–496.

PEUBE, J. L. & KREITH, F. 1966 Ecoulement permanent d'un fluide visquex incompressible entre deux disques parallèles en rotation. *J. Mécanique*, **5**, 260–286.

RICE, W. 1963 An analytical and experimental investigation of multiple disk pumps and compressors. *J. Engng for Power*, **85**, 191–200.

SAVAGE, S. B. 1964 Laminar flow between parallel plates. *J. Appl. Mech.* **86**, 594–596.

SCHLICHTING, H. 1968 *Boundary Layer Theory*, 6th edn.: McGraw-Hill.